The Quantum Point Contact Spin Filter

M. J. Gilbert* and J. P. Bird**

Department of Electrical Engineering and Center for Solid State Electronics Research,
Arizona State University, Tempe, AZ 85287-5706, USA
*matthew.gilbert@asu.edu, **bird@asu.edu

ABSTRACT

We describe an electron filter that exploits the known transmission properties of quantum point contacts to allow *local* and *tunable* control of the spin polarization in a semiconductor. When properly configured, the conductance of this device gives a direct measure of the spin polarization of the carriers transmitted through it. These predictions are confirmed by numerical simulations, performed for a spin filter with realistic device parameters.

Keywords: Spin filter, spin devices, split-gate technique, quantum point contact.

1 INTRODUCTION

The possibility of exploiting the spin degree of freedom of charge carriers in novel electronic devices is an area of research activity that is currently attracting much interest. Recent theoretical proposals for *spintronic* devices span a wide range of functionality, from spin FETs that utilize the spin-orbit coupling in narrow-gap semiconductors [1], to spin-based quantum computers [2,3]. For applications such as these to be realized in practice, we may identify several critical requirements. Firstly, we need to be able to induce spin-polarized distributions of carriers in semiconductors, using solely *electrical* means. We then also need to be able to *detect* the degree of this polarization, once again using an electrical measurement. Finally, for some applications, it may even be desirable to *vary* the degree of polarization, and to generate it at *local* points within an electrical circuit. In this report, we propose a design for a tunable spin filter that should allow these tasks to be performed in practice. The filter is based upon the *quantum point contact* [4-7], a quasi-one dimensional electron waveguide whose width is comparable to the Fermi wavelength. By studying transport through a realistic filter, we discuss the requirements that must be satisfied to successfully implement such a device.

2 THE QUANTUM POINT CONTACT SPIN-FILTER

The proposed spin-filter is illustrated schematically in Fig. 1, in which the structure is shown in a cross-sectional view. The basic idea of operation is that the lower set of

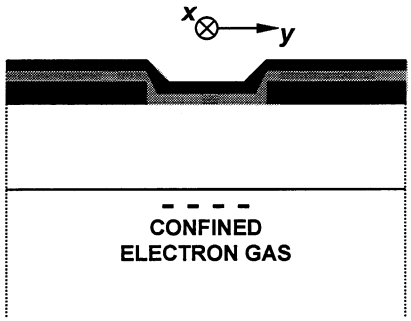

Figure 1: Schematic illustration of the proposed spin filter. The black regions correspond to metallic gates, while the gray shading denotes a thin insulating layer. The coordinate system is also indicated for reference.

split gates is used to define a quantum point contact in the high-mobility two-dimensional electron gas of a suitable heterostructure [4,5]. (The choice of heterostructure system will turn out to be crucial for the successful implementation of the spin filter, a point we return to in detail below.) The lower split gates are separated from an upper *continuous* gate by a thin insulating layer, which may be realized in practice by oxide deposition or by hardening of electron-beam resist [8]. To operate the structure as a spin filter, the lower split gates are first configured such that the point contact lies close to its threshold for conduction. By driving a steady current through the upper gate, a local magnetic field is then generated that lifts the spin degeneracy of the carriers and causes preferential transmission of one spin species through the point contact. By measuring the conductance of the point contact as the current in the upper gate is varied, we show below that it should be possible to determine the spin polarization of the transmitted carriers.

3 THEORETICAL MODEL FOR THE SPIN FILTER

To model the response of the proposed spin filter we begin by recalling the results of magneto-transport studies in quantum point contacts [4-7], which have demonstrated that a magnetic field may be used to induce the selective depopulation of spin-resolved subbands. For a quantitative description of this depopulation, the potential profile in the point contact may be modeled with a saddle-like form [6,7]:

$$V(x,y) = V_o - \frac{1}{2}m^*\omega_x^2 x^2 + \frac{1}{2}m^*\omega_y^2 y^2. \quad (1)$$

In this equation, the x and y directions are taken to lie along and perpendicular to the axis of the quantum point contact, respectively (Fig. 1). V_o is the height of the saddle-barrier, m^* is the electron effective mass, and $\omega_{x,y}$ are characteristic oscillator frequencies. ω_y determines the energy splitting of the one-dimensional sub bands in the point contact, while ω_x defines the width of the tunnel barrier formed by the saddle potential. In a magnetic field applied perpendicular to the plane of the contact, the transmission coefficients of the one-dimensional subbands may be written as [9,10]:

$$T_n = \frac{1}{1+\exp(-\pi\varepsilon_n)}. \quad (2)$$

Here, n is the usual harmonic-oscillator index (n = 0, 1, 2, 3, ...) and ε_n is defined as:

$$\varepsilon_n = \frac{E - E_2(n+1/2) - V_o}{E_1}, \quad (3)$$

where E is the energy of the incoming carriers and the parameters E_1 and E_2 are defined via:

$$E_1 = \frac{\hbar}{2\sqrt{2}}([\Omega^4 + 4\omega_x^2\omega_y^2]^{0.5} - \Omega^2)^{0.5}, \quad (4)$$

$$E_2 = \frac{\hbar}{\sqrt{2}}([\Omega^4 + 4\omega_x^2\omega_y^2]^{0.5} + \Omega^2)^{0.5}. \quad (5)$$

In Equations (4) & (5), Ω is a magnetic-field (B) dependent oscillator frequency, $\Omega^2 = \omega_c^2 - \omega_x^2 + \omega_y^2$, and the cyclotron frequency $\omega_c = eB/m^*$.

The idea of the spin filter is to exploit the spin-dependent tunneling probabilities that exist for a potential barrier in the presence of a magnetic field. This magnetic field induces a Zeeman splitting $\pm\frac{1}{2}g\mu_B B$ of the electron energy, where g is the effective g-factor, and μ_B is the Bohr magneton. For an electron with an initial energy E at zero field, we may use Equations (2) – (5) to define *separate* transmission probabilities for its spin components in the presence of a magnetic field:

$$T_\pm(E, B) = T(E \pm \tfrac{1}{2}g\mu_B B). \quad (6)$$

4 MODELING RESULTS

To illustrate the response of the spin filter, in Fig. 2 we model a device whose potential parameters correspond to those of a typical point contact that is biased close to pinch off [7]. For simplicity, we have assumed here that the g-factor takes the free-electron value (g = 2) and that the electron effective mass is that for GaAs ($m^* = 0.067m_o$). In Figs. 2(a) & 2(b), we plot the variation of the spin-resolved transmission probabilities (T_+ & T_-) with magnetic field and energy. The energy range considered here is deliberately chosen to correspond to that for which the conductance is dominated by the contribution from the first subband (n = 0) alone. In Fig. 2(c), $T_+ - T_-$ is plotted for the same energy range and the gray region corresponds to the range of parameter space for which spin-filtering is effective. For an initial energy of 16.7 meV (dotted line in Fig. 2(c)), for example, strong polarization of the transmitted carriers is obtained at magnetic fields of order 0.9 T. This can be seen more clearly in Fig.3, where we plot conductance (defined as $G = (e^2/h)(T_+ + T_-)$ from the Landauer formula) as a function of magnetic field for this initial energy. We also show the variation of the spin polarization, which we define as $P = (T_+ - T_-)/(T_+ + T_-)$. In this case we see that the conductance provides a direct measure of the polarization of the transmitted carriers. At zero magnetic field, the

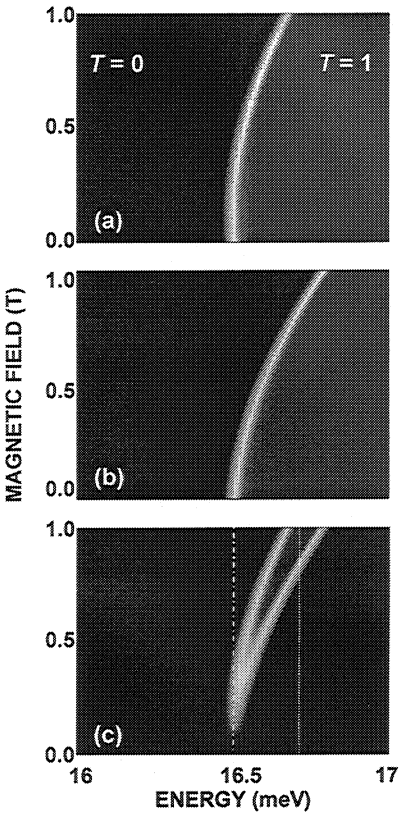

Figure 2. (a) T_+ versus energy and magnetic field. (b) T_- versus energy and magnetic field. (c) $T_+ - T_-$ versus energy and magnetic field. We have assumed V_o = 15 meV, $\hbar\omega_y$ = 3 meV and $\hbar\omega_x$ = 0.1 meV. Black regions correspond to T = 0, gray regions to T = 1, and the lighter regions denote the transition between these two levels.

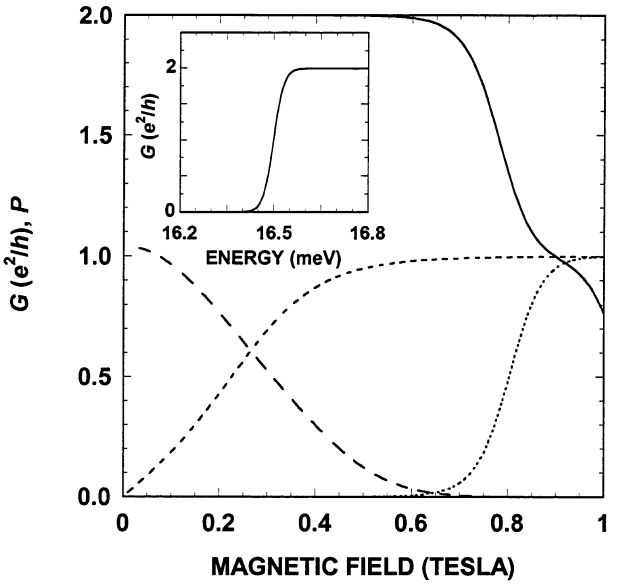

Figure 3: Variation of the conductance and polarization of the spin filter as a function of magnetic field. Solid and dotted lines indicate the variation of G and P, respectively, at an energy of 16.7 meV. Long- and short-dashed lines show the variation of G and P, respectively, at an energy of 16.5 meV. The inset shows the variation of G as a function of energy at zero magnetic field.

conductance is $2e^2/h$, since both spin components of the first subband are initially fully transmitted. As the magnetic field is increased, however, the spin polarization ultimately becomes complete. As can be seen from Fig. 3, the onset of full polarization is indicated directly in the conductance, which drops to e^2/h as P approaches unity.

A potential problem with the spin filter is that careful configuration of the quantum point contact is required to obtain a clear correlation between conductance and the degree of spin polarization. We illustrate this point in Fig. 3, where we plot the variation of G and P with magnetic field for an initial energy of 16.5 meV (dash-dotted line in Fig. 2(c)). For this initial energy, full polarization is found for a magnetic field of order 0.5 T, but the problem is that there is now *no* clear indication of this in the conductance. In fact, the polarization is induced at the expense of the transmission of *both* spin species [11]. For the successful operation of this device, we not only require a high degree of polarization, but also require the transmission of the preferred spin species be close to unity. In experiment, the actual control parameter that is varied is the split-gate voltage, rather than the energy, which sets the height of the saddle barrier (V_o). To implement the spin filter in practice, it will therefore likely be necessary to raster the split-gate voltage while searching for a conductance response similar to that shown as the solid line in Fig. 3.

A related issue to that discussed above concerns the sensitivity of the spin filtration to the *shape* of the potential

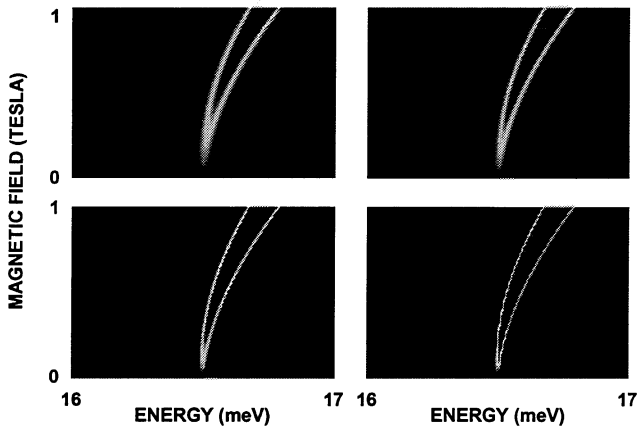

Figure 4: The influence of ω_x on the spin-filtration characteristic (T_+ - T_-). In these calculations, the barrier parameters are the same as those in Fig. 2, except ω_x is varied. Top left panel: $\hbar\omega_x = 0.07$ meV. Top right panel: $\hbar\omega_x = 0.05$ meV. Bottom left panel: $\hbar\omega_x = 0.03$ meV. Bottom right panel: $\hbar\omega_x = 0.01$ meV.

barrier formed by the quantum point contact. This effect can easily be investigated within the context of our simple model, by changing the values of the oscillator frequencies that define the shape of the saddle potential. In Fig. 4, we show the effect of varying ω_x, which characterizes the slope of the saddle potential in the direction of current flow, on the spin filter action. Reducing ω_x corresponds to increasing the *length* of the tunnel barrier in the direction of current flow and thus should yield a *sharper* tunneling threshold. This is exactly what we see in Fig. 4, where the region of spin filtration becomes more clearly defined as ω_x is reduced. It is interesting, however, that the central region of spin filtration is not significantly affected by the variation of ω_x, indicating that the device is relatively robust to variations in the length of its tunnel barrier. Variation of the oscillator frequency ω_y turns out to be even less critical for device application, as we illustrate in Fig. 5. This parameter sets the potential variation in the direction *transverse* to the current flow and thus determines the spacing of the one-dimensional subbands in the point contact [9]. In this sense, we may consider that ω_y, in combination with the barrier height, defines an energy threshold for conduction via a given subband. As we increase the value of ω_y, we drive this threshold to higher energy and so shift the spin-filter region *wholesale* to higher energies, as shown in Fig.5.

5 DISCUSSION

The preceding analysis suggests that local magnetic fields of order 1 T are required to induce sufficient splitting of two spin components in the system modeled here. For a typical separation of 100 nm between the upper gate and

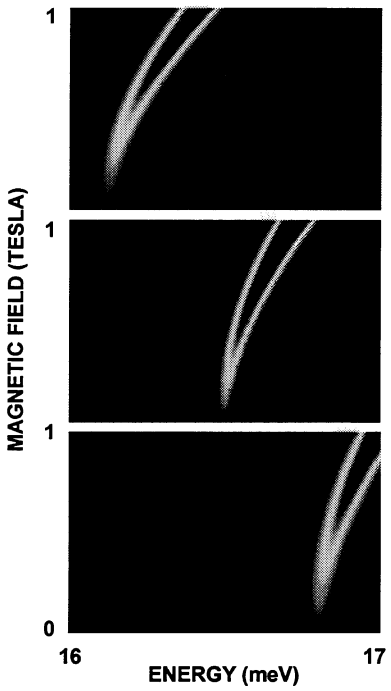

Figure 5: The influence of ω_y on the spin-filtration characteristic (T_+ - T_-). In these calculations, the barrier parameters are the same as those in Fig. 2, except ω_y is varied. Top panel: $\hbar\omega_y = 2.25$ meV. Middle panel: $\hbar\omega_y = 3$ meV. Bottom panel: $\hbar\omega_y = 3.6$ meV.

the electron gas, this requires a drive current of roughly 500 mA if the gate is modeled as a microstrip 50 nm wide [12]. While the required drive current may be reduced significantly by decreasing the separation between the electron gas and the upper gate, a more fruitful approach will be to exploit heterostructures with strongly enhanced g-factors. In InAs, for example, the g-factor is –15, while in InSb it is as large as –51 [13]. Using the heterostructures of these materials [14,15], it should be possible to achieve the desired polarization at much lower magnetic fields, even in the mT range. A more serious issue is the high temperature operation of the spin-filter. For the highest fields considered here, the magnitude of the spin splitting is not much more than a degree Kelvin. The use of high g-factor substrates should increase this splitting by more than an order of magnitude, however, and so greatly extend the temperature range of operation. Finally, while in our discussion we have focused on the use of the filter as a means of generating spin polarized carriers, it is clear that this device should also allow for *detection* of spin polarized carriers.

6 CONCLUSIONS

In conclusion, we have proposed a tunable spin filter that exploits the ballistic nature of transport in quantum point contacts to provide spin polarization of incident carriers. The filter should allow for local and tunable control of the spin polarization in a circuit, and should also allow detection of the spin state of carriers incident upon it. The basic filter action appears to be relatively robust to the presence of variations in the shape of its potential profile, although careful configuration is required in order to obtain a clear signature of the spin polarization in the conductance. The structure we have proposed should be relatively easy to fabricate using standard electron-beam techniques, although the use of high g-factor material appears to be crucial to its successful implementation.

Acknowledgements: This work was supported by the Office of Naval Research. The authors would particularly like to acknowledge invaluable discussions with R. Akis.

REFERENCES

[1] S. Datta and B. Das, Appl. Phys. Lett. **56**, 665 (1990)

[2] D. Loss and D. P. DiVincenzo, Phys. Rev. A **57**, 120 (1998).

[3] G. Burkard, D. Loss and D. P. DiVincenzo, Phys. Rev. B **59**, 2070 (1998).

[4] B. J. van Wees, H. van Houten, C. W. J. Beenakker, J. G. Williamson, L. P. Kouwenhoven, D. van der Marel, and C. T. Foxon, Phys. Rev. Lett. **60**, 848 (1988).

[5] D. A. Wharam, T. J. Thornton, R. Newbury, M. Pepper, H. Ahmed, J. E. F. Frost, D. G. Hasko, D. C. Peacock, D. A. Ritchie, and G. A. C. Jones, J. Phys. C **21**, L209 (1988).

[6] H. van Houten, C. W. J. Beenakker, and B. J. van Wees, in *Semiconductors and Semimetals*, edited by M. A. Reed (Academic Press, New York, 1992), p. 35.

[7] B. J. van Wees, L. P. Kouwenhoven, E. M. M. Willems, C. J. P. M. Harmans, J. E. Mooij, H. van Houten, C. W. J. Beenakker, J. G. Williamson, and C. T. Foxon, Phys. Rev. B **43**, 12431 (1991).

[8] I. Zailer, J. E. F. Frost, V. Chabasseur-Molyneux, C. J. B. Ford, and M. Pepper, Semicond. Sci. Technol. **11**, 1235 (1996).

[9] M Büttiker, in *Semiconductors and Semimetals*, edited by M. A. Reed (Academic Press, New York, 1992), p. 191.

[10] H. A. Fertig and B. I. Halperin, Phys. Rev. B **36**, 7969 (1987).

[11] M. J. Gilbert and J. P. Bird, Appl. Phys. Lett. **77**, 1050 (2000).

[12] K. R. Demarest, *Engineering Electromagnetics* (Prentice Hall, NJ,1998).

[13] K. Seeger, *Semiconductor Physics*, 7th Edition (Springer-Verlag, Berlin, 1999).

[14] S. J. Koester, C. R. Bolognesi, M. Thomas, E. L. Hu, H. Kroemer, and M. J. Rooks, Phys. Rev. B **50**, 5710 (1994).

[15] Y.–H. Zhang, J. Cryst. Growth **150**, 838 (1995).